International Journal of Biological Macromolecules 170 (2021) 24–32

Contents lists available at ScienceDirect

International Journal of Biological Macromolecules

journal homepage: http://www.elsevier.com/locate/ijbiomac

Cellulose nanocrystals based clove oil Pickering emulsion for enhanced antibacterial activity

Huaping Yu [a,1], Guiting Huang [a,1], Yueqin Ma [b], Yang Liu [a], Xiaoying Huang [a], Qin Zheng [a], Pengfei Yue [a,c,*], Ming Yang [a]

[a] Key Lab of Modern Preparation of TCM, Ministry of Education, Jiangxi University of Traditional Chinese Medicine, 1688 Meiling Avenue, Nanchang 330004, China
[b] Department of Pharmaceutics, 908th Hospital of People's Liberation Army, Nanchang, China
[c] Australian Institute for Bioengineering and Nanotechnology, The University of Queensland, Brisbane, QLD 4072, Australia

ARTICLE INFO

Article history:
Received 28 August 2020
Received in revised form 8 November 2020
Accepted 4 December 2020
Available online 29 December 2020

Keywords:
Cellulose nanocrystals
Pickering emulsion
Rough surface
Clove essential oil
Antibacterial activity

ABSTRACT

An effective antibacterial system was developed by using clove essential oil Pickering emulsion (CO-PE). The carboxymethyl cellulose sodium modified cellulose nanocrystals (CNC) was used as the stabilizer of CO-PE, which were prepared by environmentally friendly approach of homogenization technology. The factors affecting the formation and stability of CO-PE were studied, such as CNC concentration, homogenization pressure, CO concentration and ionic concentration and pH. And the antibacterial performance of CO-PE against *E. coli* and *S. aureus* was investigated by determining the minimal inhibitory concentration (MIC). The results showed that 1% CNC stabilized CO-PE exhibited small droplet size and rough surface, and had good stability at high pH values or salt concentration, owing to the presence of CNC on interface of droplet. And the CNC-stabilized CO-PE exhibited higher antimicrobial activity at equivalent CO concentration, which might be attributed to efficiently adhere to bacterial membrane. Therefore, our research would provide new insights for antibacterial application of Pickering emulsions loading essential oils in the food and other industries.

1. Introduction

Bacterial infection has been a major threat to human health, especially with increasing levels of antimicrobial resistance in recent decades [1]. Conventional antibiotics have caused multidrug resistance and side effects owing to the long-term use and overuse. The development of new antibiotics or formulations is posing urgent challenges [2]. The essential oil are known for their antibacterial, antifungal, antiviral, antioxidant, and biological modulation properties [3,4], which has been widely used in the food, perfumes, cosmetic, and pharmaceutical industries [5]. Clove oil (CO) (*Eugenia caryophyllata*; Myrtaceae) as well known essential oil containing several active components such as eugenol and caryophyllene exhibits several biological activities as an anti-inflammatory [6], antioxidant [7] and antibacterial effect [8]. However, the use of CO in industry was strictly hindered owing to its irritation towards the mucosa and skin, its pungent taste, light sensitivity, volatility and poor water solubility [9]. Furthermore, owing to the low water solubility and hydrophobicity, the essential oil likely remains on the surface of the bacteria medium and cannot effectively interact with bacteria. These can strictly limit the antibacterial efficiency of essential oil.

To tackle these problems, many strategies have already been developed by different encapsulation methods, such as microcapsulation, microsphere, and nanoparticles [10–12]. Pickering emulsion is thought to be effective strategy for encapsulation and antibacterial application of essential oil [13–15]. Compared with the conventional emulsions, Pickering emulsion is a new type of emulsion stabilized by solid particles instead of surfactants. Meanwhile, it shows an excellent emulsion droplet stabilization, owning to the nearly irreversible adsorption of solid particles at the oil-water interface. Thus, Pickering emulsion is stable enough to protect the core materials in the microencapsulation procedure. As a result, it has attracted increasing interest in encapsulation of the essentials oils.

Notably, the surface roughness of nanocarrier has been widely recognized as a key feature influencing the surface-bacteria interactions, and nanoscale surface roughness can enhance bacterial attachment [16,17]. Hao et al. designed the mesoporous silica nanospheres with rough surfaces, which showed enhanced adhesion towards bacteria surfaces compared to their counterparts with smooth surfaces [18]. Thus the Pickering emulsions exhibited the rough surface due to the coverage of solid nanoparticle in droplet interface. And the surface topography of Pickering emulsions droplet could be shaped

* Corresponding author at: Jiangxi University of Traditional Chinese Medicine, 1688 Meiling Avenue, Nanchang 330004, China.
E-mail address: feigleyue@outlook.com (P. Yue).
[1] Huaping Yu and Guiting Huang contributed to the work equally as joint first authors.

https://doi.org/10.1016/j.ijbiomac.2020.12.027
0141-8130/

by regular or irregular nanoparticles in the interface [19]. Ma and colleagues developed a poly (lactic-*co*-glycolic acid) (PLGA) nanoparticles stabilized Pickering emulsions adjuvant system(PPAS), and demonstrated that the PPAS resulted in the increased surface contact at the droplet–cell interface owing to the pliability and mobility of solid particles [20]. This could be hypothesized that the Pickering emulsions could enhance adhesion towards the bacterial surface and thus improve the antibacterial efficacy of the essential oils. Therefore, Pickering emulsion can not only improve stabilization and dispersibility of essential oils, but also thus enhance the antimicrobial ability of essential oils. But as so far, there is no report on the adjuvant effect of surface roughness of Pickering emulsion loaded essential oils on their antibacterial performance.

In this study, CO was used as oil phase, a novel Pickering emulsion with a rough surface(CO-PE) was designed, using carboxymethyl cellulose sodium modified cellulose nanocrystals (CNC) as stabilizer. CNC was regarded as ideal solid particles of Pickering emulsion due to their needle-shaped nanocrystals, low density, chemical tenability, and environmental sustainability. The novel aspect of the current work exhibited that the CNC stabilized CO-PE could have the strong antibacterial activity against *E. coli* and *S. aureus*, dependent on the enhanced adhesion and encapsulated CO. Therefore, the objectives of this manuscript are as follows: (1) carboxymethyl cellulose sodium modified cellulose nanocrystals (CNC) was prepared by means of homogenization. The particle size, morphology and crystals state of CNC was evaluated, respectively. (2) the CNC-stabilized CO Pickering emulsions (CO-PE) were prepared by homogenization technology. The particles size, stability and morphology of CO-PE were evaluated. (3) the antibacterial activity of CO-PE was further investigated towards *E. coli* (gram negative) and *S. aureus* (gram positive), in comparison with those of free CO and CO submicron emulsions.

2. Material and methods

2.1. Materials

Microcrystalline cellulose (MCC) was commercially obtained from Fengli Jingqiu Pharmaceutical Co., Ltd. (Beijing, China). Carboxymethyl cellulose sodium (CMC-Na) was purchased from Chineway Pharmaceutical Co., Ltd. CO (the content of eugenol more than 60%) was kindly supplied by Jian Tian Yuan Medical Oil Refinery (Jiangxi, China). Nile Red and Nile Blue A were purchased from Shanghai Yuanye Bio-Technology Co., Ltd. (Shanghai, China).

2.2. Preparation of CNC

The carboxymethyl cellulose sodium modified cellulose nanocrystals (CNC) was prepared according to Xie et al. [21]. Briefly, 1 g MCC and 0.1 g CMC-Na were dispersed in the 100 ml water at 1000 rpm for 30 min. The gained coarse suspensions were homogenized at high pressure using a piston-gap high pressure homogenizer (AH-1000D, ATS Engineering Inc., Seeker, Canada). Firstly, 30 cycles at 200 bar, 20 cycles 500 bar were conducted as pre-milling step, and afterwards, 30 cycles at 1000 bar were run to obtain the CNC dispersions. The CNC was finally obtained after freeze-drying at −40 °C.

2.3. Preparation of CO-PE stabilized by CNC

The CO-PE was prepared by homogenization method. In briefly, different amounts of CNC (10, 25 and 50 mg) were added to 9 ml deionized water, respectively. The CNC suspensions were used as water phase. 1 ml CO was used as oil phase. The coarse CO Pickering emulsions (CO-PE) were prepared via a high-shear homogenizer (FLUKA® FA25, Essen, Germany) for 1 min at 22,000 rpm at room temperature. Then, the CO coarse emulsions was homogenized using an AH100D high-pressure homogenizer (ATS Engineering Inc., Shanghai, China) at 100 bar and 200 bar for 10 cycles, followed by 30 cycles at 800 bar pressure, with a water cooling cycle apparatus (ATS Engineering Limited, Suzhou, China) that was used to maintain the temperature of the emulsions at room temperature. Then, the CO-PE was harvested.

2.4. Crystal state of CNC

The crystal state of the coarse MCC and CNC was determined using PXRD (PANalytical, Westborough, MA, USA), respectively. The samples were scanned for 2θ ranging from 5° to 90° at a scan rate of 0.2 °C/min. Measurements were performed at a voltage of 40 kV and 25 mA.

2.5. Fourier transfer-infrared (FT-IR) spectroscopy of CNC

The IR spectra of MCC and CNC was determined by means of Fourier transform infrared spectrophotometry (FT-IR Spectrometer, BRUKER IFS-55, Switzerland), respectively.

2.6. Particle size and zeta potential measurements of CNC and CO-PE

The particles size determination of CNC suspensions and CO-PE was performed on a Mastersizer Micro Plus (Malvern Instruments Limited, Worcestershire, UK). Analysis of the diffraction patterns was done using the Mie model ("standard" presentation: dispersant refractive index = 1.33, real particle refractive index = 1.53, imaginary particle refractive index = 0.1). The surface mean droplet diameter ($D_{3,2}$) of each sample was represented as the mean diameter, which was related to the specific surface area of the oil droplets. All measurements were performed in triplicate.

The Zeta potentials of CNC suspensions and CO-PE were determined by the dynamic light scattering (Nano ZS, Malvern instrument). The samples were firstly diluted to a concentration of approximately 0.05% (w/w) using deionized water in order to avoid multiple scattering effects. All measurements were performed in triplicate. The Zeta potential was recorded as the average and standard deviation of measurements.

2.7. Emulsion morphology of CO-PE

The morphology of the CO-PE was analyzed by transmission electron microscopy (TEM) (JEM-1200EX; JEOL, Tokyo, Japan). The samples were diluted in distilled water and placed on a copper grid. The grid was dried at room temperature and was evaluated with the electron microscope.

The CO-PE was also observed by confocal laser scanning microscopy (CLSM) (LSM 710, Germany). The Nile Red dye was used to stain oil phase and Nile Blue A was applied to stain CNC. The tested CO-PE was dyed with a mixed fluorescent dye solution consisting of 1 mg ml^{-1} Nile Red and 1 mg ml^{-1} Nile Blue A. The dyed CO-PE was put on concave slides, and then the concave slides were covered with coverslips. Finally, glycerol was coated around the coverslips to seal the samples. The fluorescent dyes were excited by either an argon laser at 543 nm for Nile Red or a helium neon (He—He) laser at 633 nm for Nile Blue A [22].

2.8. Surface coverage

The percentage surface coverage (C) of the CNC-stabilized droplets was calculated according to the previous descripted method [23]:

$$C = 100 \times \frac{m_p D_{32}}{6h\rho V_{oil}}$$

where m_p was the mass of adsorbed CNC (kg), D_{32} was the mean droplet diameter (m), h was the thickness of the adsorbed CNC layer (m), ρ was the density of CNC (1400 kg/m^3), and V_{oil} was the volume of CO in the emulsion (m^3). The thickness of the CNC layer was 8 ± 3 nm [21].

2.9. Emulsion stability

The freshly prepared CO-PE containing 1 wt% CNC and 10 wt% CO was subjected to a series of environmental stresses including a range of pH and ionic strength conditions. Thermal processing: CO-PE (10 ml) were filled into glass tubes and incubated in water baths (30–90 °C) for 30 min, and then naturally cooled to ambient temperature. The pH and ionic strength were set as follows: the CO-PEs were placed in 20 ml beakers, adjusted to investigated pH values (2−10) using NaOH and/or HCl solutions or salt levels (100–500 mM) by adding NaCl, and then transferred into glass tubes.

2.10. Inhibition activity of minimum inhibitory concentration (MIC)

A series of concentrations of CO were investigated to study the antibacterial activity of free CO and CO-PE. 100 μl of bacterial suspension (1×10^7 CFU mL^{-1}) was added into 800 μl of LB medium in 1.5 ml centrifuge tube. 100 μl of samples (CO and CO-PE) in PBS at different CO concentration was added respectively into the mixture with PBS only as the control group. Then the mixture was shaken on a shaker at 37 °C at 200 rpm for 24 h. The multifunctional microplate reader (infinite M200, Tecan) was used to measure OD at 600 nm and the samples in the absence of bacteria were recorded as background to remove turbidity resulted from CO-PE and CO. The percentage of OD reading of samples (subtracted background) to PBS group presented the bacterial viability. Every concentration was prepared in triplicates.

LB-agar plates assay was used to further confirm antibacterial activity before and after 24 h of the above treatment. 20 μl of bacteria suspensions were spread on sterilized plates with LB-agar medium and incubated at 37 °C overnight.

The bacteria colonies grown in each plate were observed and the images were taken.

3. Results and discussions

3.1. Characterization of CNCs

Different from sulfuric acid hydrolyzed method [24], a stable CNC modified by carboxymethyl cellulose sodium (CMC—Na) was prepared from microcrystalline cellulose (MCC) by homogenization technology. At process of homogenization, the surface energy of CNC was remarkably increased with the decrease of particle size of CNC, and nanosized CNC particles could easily generate flocculation, aggregation or crystal growth to decrease their free energy. Therefore, co-processed modification of CNC particles with water soluble polymers has also recently gained increasingly interest for successful production of colloidal formulation [21,24–27]. In this study, the carboxymethyl cellulose sodium modified cellulose nanocrystals (CNC) could be easily produced by homogenization. The CNC seemed to be rod-like particles with mean particle size that had typical dimensions of around 5–10 nm in width and 112.3 ± 2.5 nm in mean length, and exhibited the excellent homogeneity and stability, as shown in Fig. 1A and B.

The XRD diffractograms of raw MCC and CNC were shown in Fig. 1C. Raw MCC exhibited the characteristic peaks at 2θ of 16.4, 22.5 and 35.6° (Fig. 1C). These were consistent with the previous report [28]. The CMC-Na-modified CNC exhibited the crystalline characteristic peaks of MCC, and the characteristic peak of CMC-Na at 2θ of 21.7°. There still existed the characteristic peak of MCC and CMC-Na at the same 2θ position indicating that the crystal state of CNC was not changed during homogenization.

The infrared spectra of MCC and the CNC were shown in Fig. 1D. Fig. 1D showed the characteristic absorption peak of MCC: OH, 3345 cm^{-1}; C—H, 2850 cm^{-1}; C-O-C-O-C, 1033–1113 cm^{-1}. Furthermore, CNC was similar with that of the MCC, and the characteristic signals at 3345 cm^{-1}, 2890 cm^{-1}, 1638 cm^{-1} and 1033–1113 cm^{-1} indicated that the presence of cellulose structure, but the peaks of CMC-Na at 3440 cm^{-1} and 1595 cm^{-1} were almost superimposable upon that of MCC. The adsorption spectrum of the mixture of MCC and CMC-Na showed the combination of MCC and CMC—Na. These results demonstrated the co-processed modification of CNC and CMC-Na in the CNC might be dependent of physical interaction, attributed to formation of Vander Waals forces or hydrogen bond [29].

3.2. The influence of CNC concentration on preparation of CNC-stabilized Pickering emulsion

The CO-PE containing 10 wt% CO and different CNC levels were homogenized at pressure of 800 bar (Fig. 2). As shown in Fig. 2A, the mean droplet diameter ($D_{3,2}$) decreased with increasing CNC concentration from 0.05 to 0.75 wt%, and the CO-PE containing 0.05 wt% CNC exhibited the relative large droplet diameter (>4 μm) before and after storage, which was probably attributed that the CNC was insufficiently covered the oil droplet surfaces during homogenization. But with increasing of CNC concentration from 0.75 to 1.25 wt%, the particle size of CO-PE reached a plateau value of ~600 nm (Fig. 2B). The particle size versus CNC concentration relationship observed therefore followed the typical two-regime profile seen for high-pressure homogenization [30]. This kind of behavior was because the size of oil droplets produced by homogenization was limited by the amount of stabilizer present at low CNC levels, but by the disruptive energy during homogenization at high CNC loadings. The particle size distribution of CO-PE was monomodal from 0.1 to 1.1 wt% CNC but bimodal at 1.2 wt% CNC (Fig. 2B). This bimodal distribution might be attributed to presence of the CO-PE and free CNC. Based on the location of the smaller peak in the particle size distribution curves (~50 nm), these small particles could be speculated to be free CNC dispersed in the aqueous phase. Moreover, the percent surface coverage of CO-PE with different CNC concentration was shown in Fig. 2A. The result shown that the calculated surface coverage values for the oil droplets were less than 80% for CNC < 0.75 wt% (Fig. 2A). This demonstrated that these CO-PE droplets with less than 0.75% of CNC seemed to not be effectively stable to coalescence during storage, owing that their surfaces were not saturated with CNC. But the calculated surface coverage values were more than 100% for CO-PE with CNC > 0.75 wt%, which suggested that either multilayers formed at the droplet surfaces or some of excess CNC was dispersed in the aqueous phase[22][23]. This indicated that the CNC nanorods were able to generate a strong electrostatic repulsion between the droplets when using CNC concentration more than 0.75 wt%.

3.3. Impact of homogenization pressure on preparation of CNC-stabilized Pickering emulsion

The size of oil droplets produced using homogenization technology was dependent on the disruptive forces generated at the operation pressure. Fig. 2 showed the influence of various homogenization pressures on the mean droplet diameter of CO-PE. Initially, the droplet diameter of CO-PE gradually decreased as the operating pressure was increased from 500 to 1000 bar (Fig. 3A), with a minimum mean droplet diameter of ~0.521 μm being achieved.

Moreover, the droplet size distributions of the CO-PE were monomodal at all pressures tested, even at the lowest (500 bar) (Fig. 3B). The span of the CO-PE also decreased from 2.5 to 1.5 with the increased homogenization pressure. This indicated that all of the oil droplets had be crushed through the disruptive zone inside the homogenizer. The decrease in droplet size with increasing pressure could be attributed to the increase in the magnitude of the crushing energy during homogenization, which could result in more efficient disruption of droplet. But the droplet diameters of CO-PE reached a plateau value of ~550 nm from 800 bar to 1200 bar. This could be attributed that the applied CNC was insufficient to cover all the very small oil droplets formed at the relatively high pressure, or because the CNC itself was damaged at relatively high pressures.

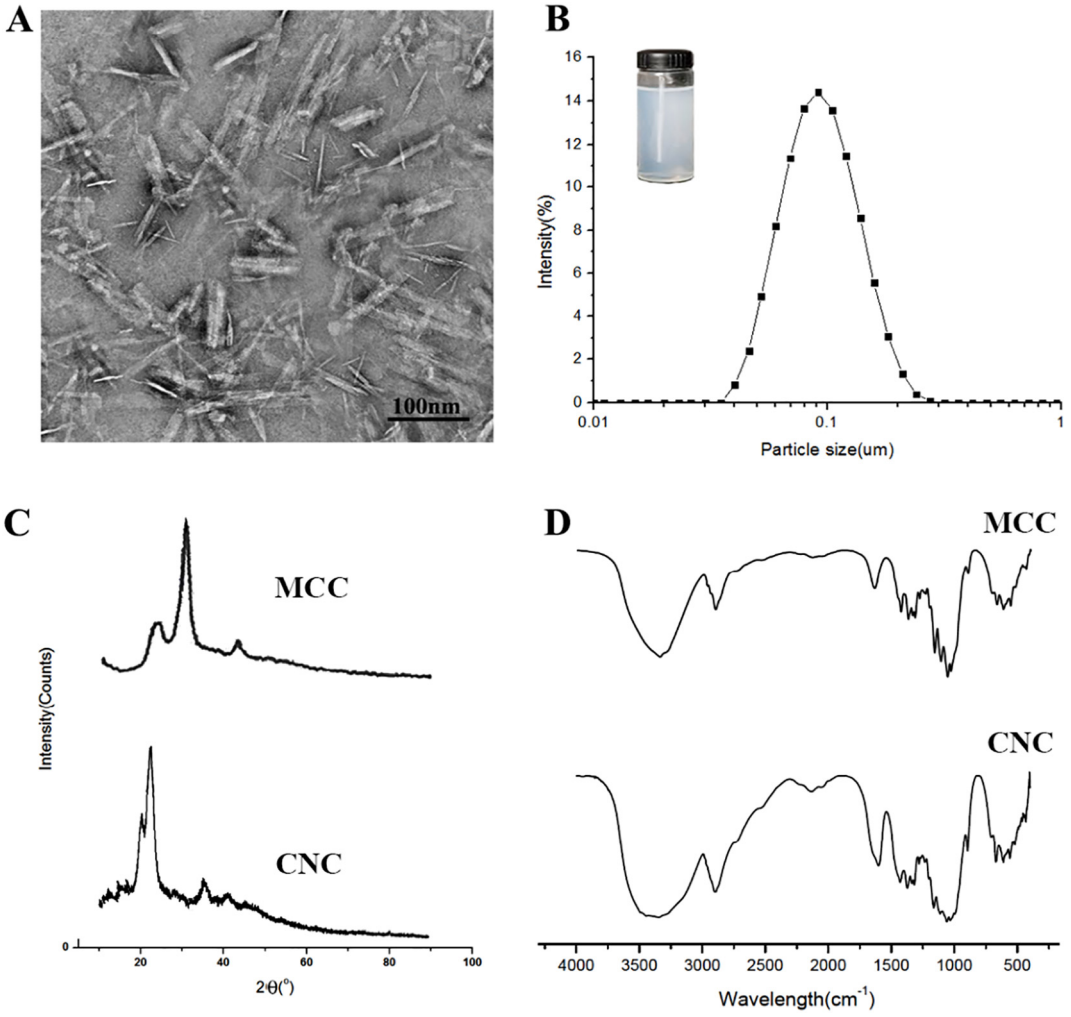

Fig. 1. TEM image (A) and mean particle size (B) of CNC, XRD diffractograms of raw MCC and CNC (C), and the IR spectrum of MCC and CNC(D).

3.4. Influence of CO concentration on preparation of CNC-stabilized Pickering emulsion formation

The oil/water ratio is a noteworthy factor affecting the Pickering emulsion stability and even the emulsion type. As it was shown in Fig. 4, the oil/water ratio had an obvious influence on the drop diameter of the CO-PE. When the CNC concentration was 1%, the average droplet diameters of the CO-PE with lower oil/water ratio (5% and 10%) were 0.516 ± 0.012 and 0.551 ± 0.023 μm, respectively. The results showed that the CO-PEs with high oil/water ratio (15% and 20%) possessed a

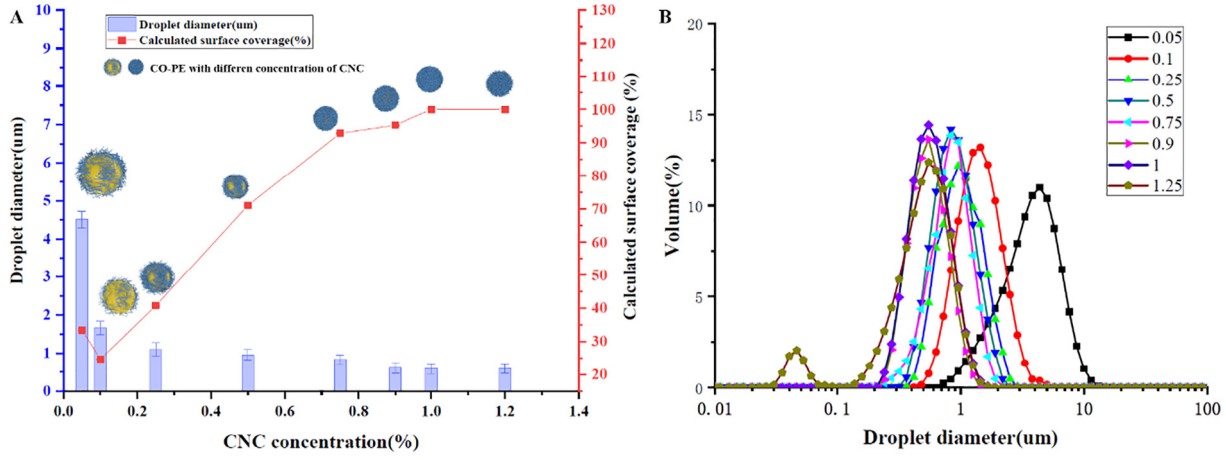

Fig. 2. The droplet diameter of CO-PE and the calculated surface coverage of CNC on the droplet surface of CO-PE(A) and the droplet size distributions of the CO-PE(B).

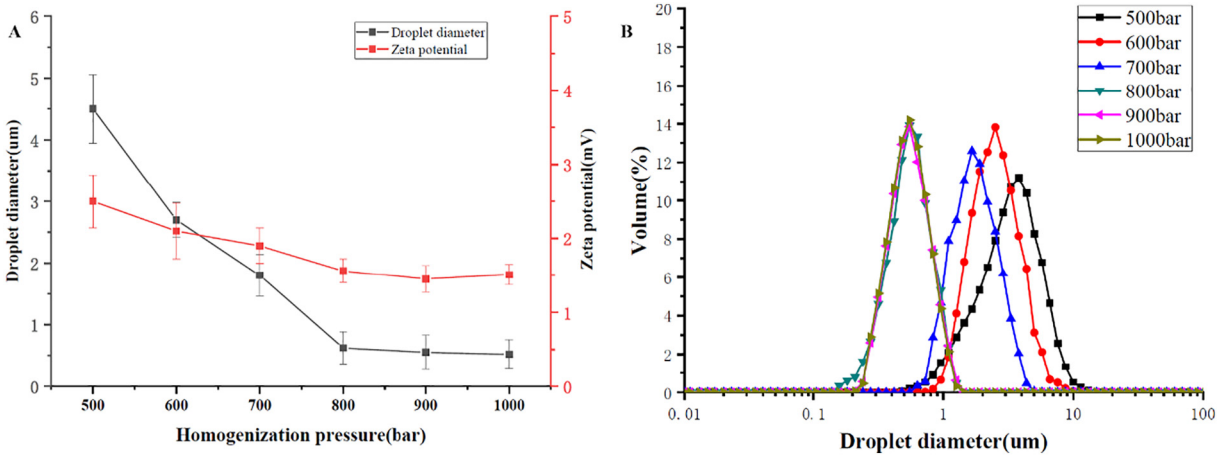

Fig. 3. Mean droplet diameter (A) and droplet size distributions (B) of CNC-stabilized CO-PE produced at different homogenization pressures.

larger droplet size as compared to those with lower oil/water ratio at the equivalent CNC concentration. Since the CNC concentration in the system was a certain number, it seemed that the addition of extra oil could increase the interfacial area which might not be sufficiently covered by the available CNC. This could result in rapidly coalescing and growing up of small drops in order to reduce the interfacial area [31,32].

3.5. Stability of CNC-stabilized Pickering emulsion

3.5.1. Thermal process

Fig. 5A showed the influence of thermal processing on the stability of Pickering emulsions. There was not remarkable change in the mean droplet diameter of the emulsions in the investigated ranges of temperatures. Moreover, no creaming or oiling-off was observed from visual appearance of the emulsions. These results suggested that the CNC-stabilized CO-PE were resistant to high temperature, which might be attributed to the strong steric or electrostatic repulsion between the droplets. The CNC-stabilized CO-PE maintained a high surface potential (−55 mV) after thermal treatment (Fig. 5A).

3.5.2. pH

Fig. 5B showed that the influence of the pH value on the stability of CO-PE. The results showed that the particle size and zeta potential of CO-PE decreased with increasing the pH value from 2 to 10. The CO-PE contained relatively small oil droplets that were visibly stable to creaming and oiling-off from pH 3 to 10. This could be attributed to the fact that the oil droplets possessed relatively strong negative potential in the investigated pH range (Fig. 5B). As a result, the droplets could be prevented from aggregation by a combination of strong electrostatic and steric repulsions. When the pH of the system was increased from 3 to 10, the surface charge decreased from −48.3 mV to −56.2 mV. So the absolute magnitude of zeta potential of CO-PE was larger, the electrostatic repulsion between droplets would become greater. As a result, the CO-PE seemed to be more stable [33]. But at pH 2, the droplet diameter of CO-PE increased remarkably, which could be attributed to a limited amount of droplet flocculation. As shown in Fig. 5A, the zeta potential of CO-PE became less negative (−24 mV) at pH 2, which might be ascribed to deprotonation of some of the protonated carboxyl groups on the CNC ($-COOH \rightarrow -COO^- + H^+$) [34]. As a result, the electrostatic repulsion between the oil droplets was not strong enough compared to the van der Waals attraction, the droplet flocculation of CO-PE occurred at pH 2.

3.5.3. Ionic strength

The influence of ionic strength on the stability of the CO-PE was investigated by incubating them at different NaCl levels (Fig. 5C). Fig. 5C also showed that the mean droplet diameter remained relatively low from 0 to 400 mM NaCl, but increased slightly at 500 mM NaCl. These

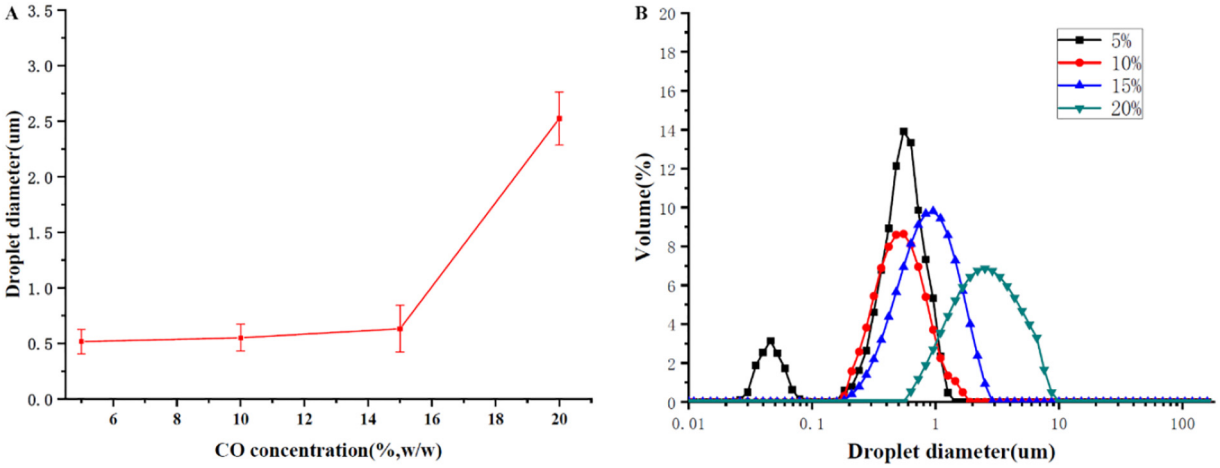

Fig. 4. Mean droplet diameter (A) and droplet size distributions (B) of CNC-stabilized CO-PE loading different concentrations of CO.

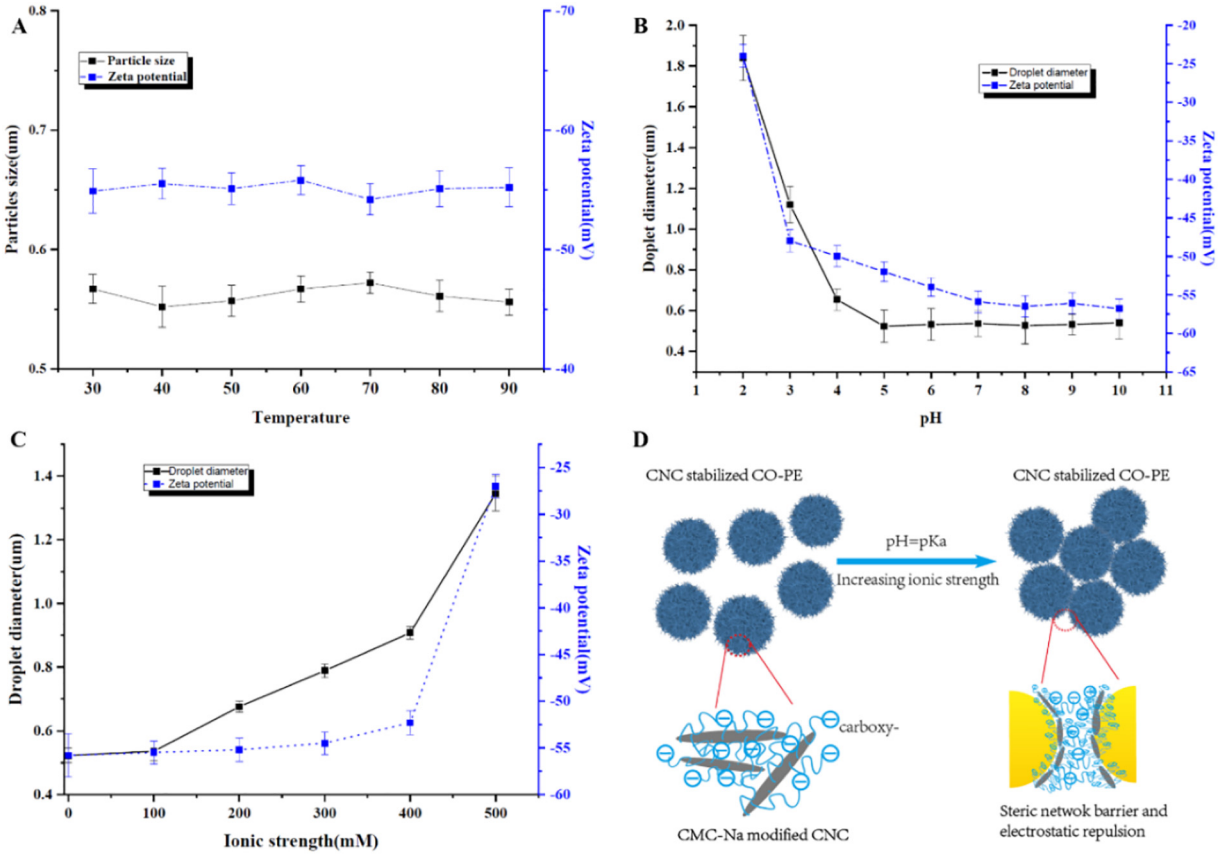

Fig. 5. The influence of (A) thermal processing temperature, (B) pH value, and (C) ionic strength on the mean particle diameter and zeta potential of CNC-stabilized CO-PE containing 10% CO.

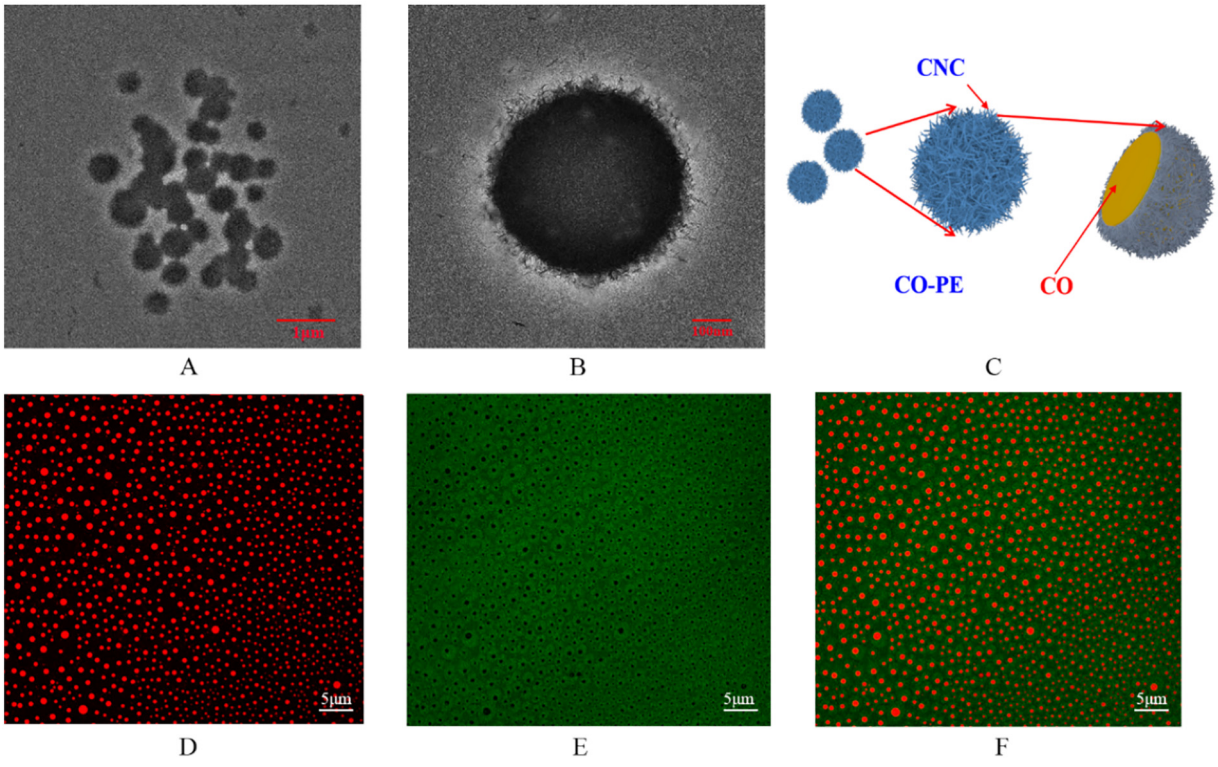

Fig. 6. TEM images of CO-PE (A, B), schematic image on configuration of CO-PE, and CLSM images of CO-PE (D Nile red, E Nile blue, F Merged)

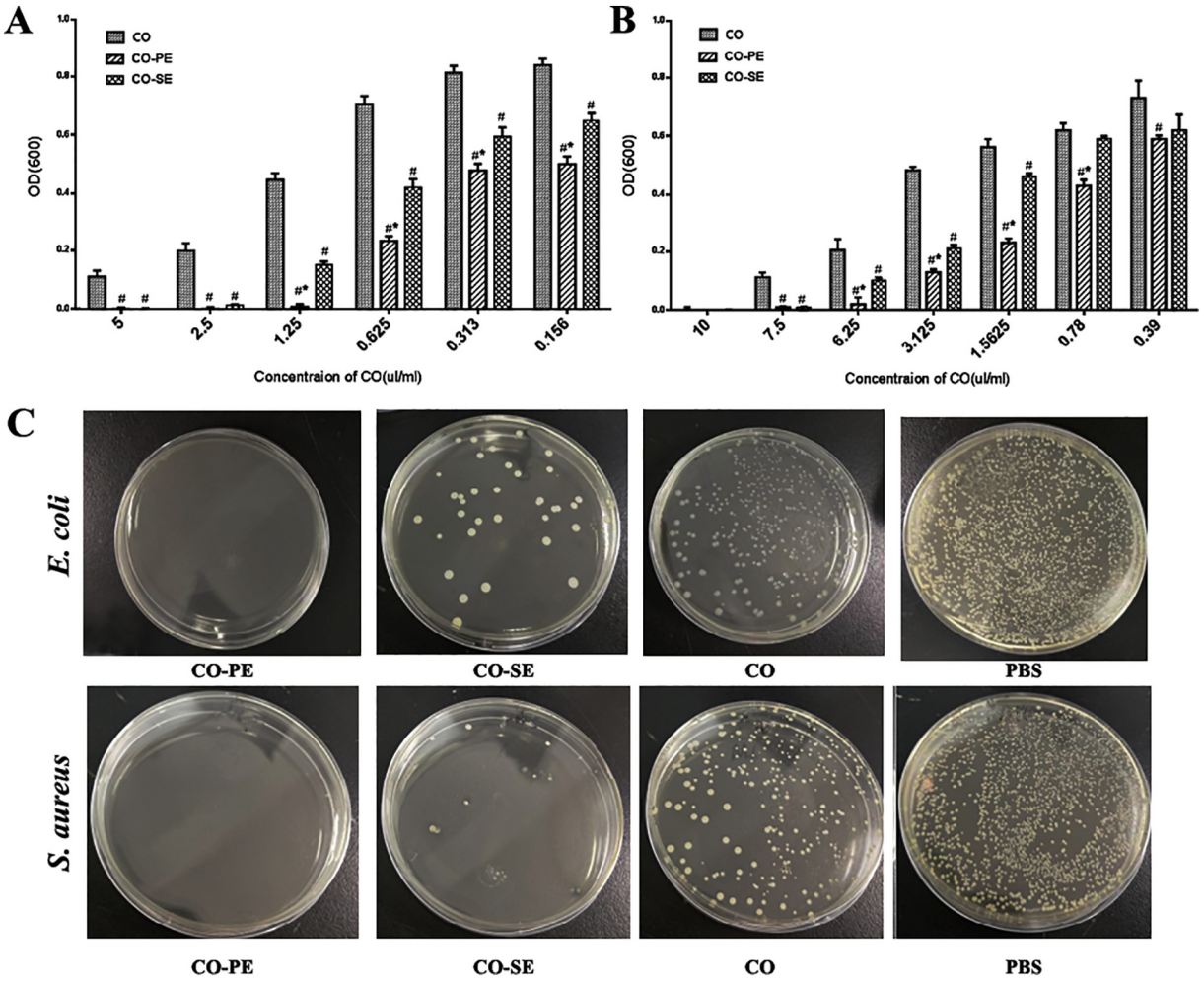

Fig. 7. Dose dependent antibacterial activities for free CO, CO-PE and CO-SE towards *E. coli.* (A) and *S. aureus*(B), and (C) Photograph of agar plates spread with bacteria suspensions containing CO-PE with concentration of 1.25 μl/ml and 6.25 μl/ml, respectively. $^{\#}p < 0.05$, compared to the free CO group; $^{*}p < 0.05$, compared to CO-SE.

results implied that the instability of the emulsions at increased ionic strength was primarily due to weak droplet flocculation rather than coalescence.

The results of zeta potential measurement (Fig. 5C) showed a steep increase (from −56.8 to −27.3 mV) in the magnitude of the surface potential with increasing ionic strength, which could be attributed to the tendency for counter-ions (in this case Na^{+}) to cluster around the surfaces of the anionic oil droplets [35]. At low ionic strength (0 and 100 mM), the electrostatic repulsion of CO-PE was sufficiently intense to overcome the van der Waals attraction, and prevent the aggregation of the oil droplets. At higher ionic strength (200–500 mM), the repulsive interactions were no longer stronger than the attractive interactions, leading the aggregation and grown up of the emulsion droplets. As shown in Fig. 5D, the tendency for droplet flocculation of CO-PE at high ionic strength could be attributed to steric barrier and electrostatic screening.

3.6. Morphology of CNC-stabilized Pickering emulsion

The TEM images of CO-PE were shown in the Fig. 6A–B. The CO-PE was sphere-shaped particle (Fig. 6A). Compared with the previous reported Pickering emulsions stabilized by individual cellulose nanocrystals [28,32,35], the CO-PE showed the small particles size of about 550 nm, which could be attributed to the effective adsorption of CMC-Na modified CNC on surface of CO-PE as well as the disintegration effect of homogenization process [21]. And the droplet surface of CO-PE seemed to be rough surface (Fig. 6B), it could be related with the presence of rod-shaped CNC particles on the oil-water interface, as illustrated in Fig. 6C. But the original CNC (Fig. 1A) seemed to be not obviously observed on the surface of CO-PE in Fig. 6B. It might be the reason that, the original CNC would be again subjected to homogenization effect during production of CO-PE, which could lead to the decrease of CNC particles size. Therefore, the morphology of the smaller CNC that covered the surfaces of Pickering emulsions seemed to not different with that of original CNC.

The morphology of the oil droplets in the CO-PE were assessed by confocal laser scanning microscopy (Fig. 5D–F). The Nile red images showed that the individual oil droplets were sphere-shaped, which demonstrated the results of TEM. The Nile blue images indicated that the CNC was mainly present in the same location as the oil droplet, which was confirmed in the merged images (the light green contour surrounding the oil droplets). This result indicated that most of CNC might be located on the oil-water interfaces.

3.7. Antibacterial activity of CNC-stabilized Pickering emulsion

The in vitro antimicrobial activity of CO-PE with rough surface was compared with those of free CO and the d-α-tocopheryl polyethylene glycol 1000 succinate (TPGS) stabilized CO submicron emulsions (CO-

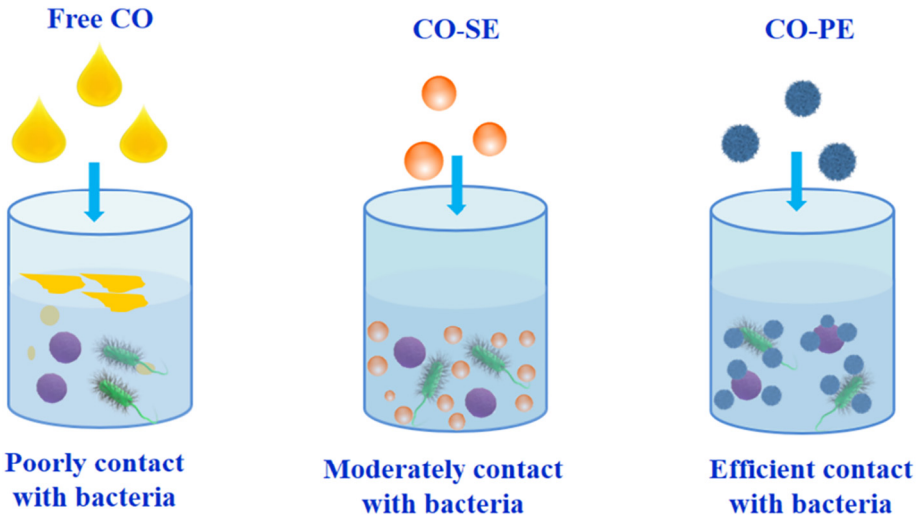

Fig. 8. Schematic images on adhesion with bacteria of free oil, CO-SE and CO-PE.

SE) with smooth surface. The CO-SE had a droplet size of 550 nm and negative zeta potential of −35 mV (TableS1).

Fig. 7 showed that free CO, CO-PE and CO-SE all exhibited dose dependent antibacterial performance towards *E. coli* (gram negative) and *S. aureus* (gram positive). As shown in Fig. 7A, the free CO exhibited limited inhibition effect towards *E. coli* even at the concentration of 5 μl/ml, as compared with CO-SE and CO-PE ($p < 0.05$). The CO-PE showed the lower OD(600) values at the lower concentration compared with CO-SE($p < 0.05$), indicating stronger antibacterial performance of CO-PE towards *E. coli* and *S. aureus*. The CO-PE had much lower MIC value of 1.25 μl/ml towards *E. coli*, in comparison with CO-SE (2.5 μl/ml) and free CO (6.25 μl/ml). As shown in Fig. 7B, the free CO exhibited the higher MIC (10 μl/ml) towards *S. aureus*, as compared with CO-PE (6.25 μl/ml) and CO-SE (7.5 μl/ml). These results also indicated that the CO exhibited the limited anti-bacterial activity towards *E. coli* and *S. aureus*, might attributed to its hydrophobicity and low water solubility in bacteria culture medium [36].

The bacterial killing activities towards *E. coli* (1.25 μl/ml of CO) and *S. aureus* (6.25 μl/ml of CO) were further evidenced by agar plate tests. Bacteria colonies grown in each agar plate were observed for PBS, free CO, CO-PE and CO-SE, in order to confirm the full inhibition of CO-PE towards *E. coli* and *S. aureus* (Fig. 7C). The difference in antibacterial activity between CO and CO-PE showed that the CO-PE could successfully enhance its antimicrobial efficacy of CO towards *E. coli* and *S. aureus*. Though the CO-PE and CO-SE had similar particle size (Table S1) and equivalent CO loading (10%), the CNC-stabilized CO-PE exhibited completely antimicrobial effect, which might be attributed to efficiently adhere to bacterial membrane (Figs. S1 and 6). Their difference in bacteria inhibition could be predominately attributed to the difference in surface morphology of particles [18]. As illustrated in Fig. 8, compared to the CO-SE with a relatively smooth surface, the CO-PE with relatively rough surface could easily attach to bacteria and cause increased local CO concentration around the bacteria, which could enhance its antibacterial activity [37]. But the free CO difficultly contacted with bacteria due to its poor diffusion ability in the culture medium.

4. Conclusions

In this study, the CO-PE with rough surface was successfully prepared by homogenization technology, using carboxymethyl cellulose sodium modified CNC as the particles stabilizer. The CO-PE was highly stable to coalescence but did exhibit flocculation and creaming. The CNC-stabilized CO-PE droplets presented good stability over a range of environmental conditions due to the steric barrier and electrostatic repulsion of CNC on the interface of emulsions droplet. Furthermore, the CO-PE showed the enhanced antibacterial activity in comparison with either CO-SE or free CO. Therefore, the rough surface structure of CNC-stabilized CO-PE offered extra advantage of enhanced adhesion towards bacteria, leading to higher antimicrobial efficacy compared to CO-SE with relatively smooth surface.

CRediT authorship contribution statement

Huaping Yu: Investigation, Formal analysis, Writing - original draft.
Guiting Huang: Formal analysis, Writing - original draft.
Yueqin Ma: Investigation, Formal analysis, Writing - original draft.
Yang Liu: Formal analysis, Writing - original draft.
Xiaoying Huang: Formal analysis.
Qin Zheng: Supervision, Formal analysis.
Pengfei Yue: Writing-Review & Editing, Supervision, Funding acquisition.
Ming Yang: Supervision, Formal analysis.

Declaration of competing interest

The authors have declared no conflict of interest.

Acknowledgements

The authors would like to acknowledge the financial support from the National Natural Science Foundation of China (81974524), and Jiangxi Science and Technology Major Project (20194ABC28009), and the youth talent support program of Jiangxi University of Traditional Chinese Medicine (1141900605). The authors acknowledge Dr. Song, Australian Institute for Bioengineering and Nanotechnology, The University of Queensland, for providing assistance.

Appendix A. Supplementary data

Supplementary data to this article can be found online at https://doi.org/10.1016/j.ijbiomac.2020.12.027.

References

[1] I. Roca, M. Akova, F. Baquero, J. Carlet, M. Cavaleri, S. Coenen, J. Cohen, D. Findlay, I. Gyssens, O.E. Heuer, G. Kahlmeter, H. Kruse, R. Laxminarayan, E. Liébana, L.

López-Cerero, A. MacGowan, M. Martins, J. Rodríguez-Baño, J.M. Rolain, C. Segovia, J. Vila, The global threat of antimicrobial resistance: science for intervention, New Microbes and New Infections 6 (2015) 22–29.
[2] SB. Levy, B. Marshall. Antibacterial resistance worldwide: causes, challenges and responses. Nat. Med. 10 (2004) S 122–129.
[3] S. Chouhan, K. Sharma, S. Guleria. Antimicrobial activity of some essential oils-present status and future perspectives. Medicines (Basel) 4(2017)58.
[4] P. Tongnuanchan, S. Benjakul. Essential oils: extraction, bioactivities, and their uses for food preservation. J. Food Sci.. 79(2014)1231–1249.
[5] J. Vergis, P. Gokulakrishnan, RK. Agarwal, A. Kumar. Essential oils as natural food antimicrobial agents: a review. Crit. Rev. Food Sci. Nutr.. 55(2015)1320–1323.
[6] K.H. Son, Kwon SY, Kim HP, Chang HW, S.S. Kang, Constituents of Syzygium aromaticum Merr. et Perry, Nat. Prod. Sci. 4 (1998) 263–267.
[7] H.C. Ou, F.P. Chou, T.M. Lin, C.H. Yang, W.H. Sheu, Protective effects of eugenol against oxidized LDL-induced cytotoxicity and adhesion molecule expression in endothelial cells, Food Chem. Toxicol. 44 (2006) 1485–1495.
[8] . Kalemba D and Kunicka A, Antibacterial and antifungical properties of essential oils. CurrMed Chem 10(2003)813–829.
[9] P. Hernández-Sánchez, S. López-Miranda, L. Guardiola, A. Serrano-Martínez, J.A. Gabaldón, E. Nuñez-Delicado, Optimization of a method for preparing solid complexes of essential clove oil with β-cyclodextrins, J. Sci. Food Agric. 97 (2017) 420–426.
[10] Chloë Maes, Sandrine bouquillon, Marie-Laure Fauconnier. Encapsulation of essential oils for the development of biosourced pesticides with controlled release: a review. Molecules. 24(2019)2539.
[11] Benavides S, Cortés P, Parada J, Franco W. Development of alginate microspheres containing thyme essential oil using ionic gelation. Food Chem.. 204(2016)77–83.
[12] Saporito F, Sandri G, Bonferoni MC, Rossi S, Boselli C, Icaro Cornaglia A, Mannucci B, Grisoli P, Vigani B, Ferrari F. Essential oil-loaded lipid nanoparticles for wound healing. Int. J. Nanomedicine 27(2017)175–186.
[13] Xu Yaoyao, Yifu Chu, Xiao Feng, Chengcheng Gao, Weiwei Cheng DiWu, Linghan Meng, Yan Zhang, Xiaozhi Tang, Effects of zein stabilized clove essential oil Pickering emulsion on the structure and properties of chitosan-based edible films, Int. J. Biol. Macromol. 156 (2020) 111–119.
[14] J.Y. Zhu, C.H. Tang, S.W. Yin, X.Q. Yang, Development and characterization of novel antimicrobial bilayer films based on polylactic acid (PLA)/Pickering emulsions, Carbohydr. Polym. 181 (2018) 727–735.
[15] H. Sun, S. Li, S. Chen, C. Wang, D. Liu, X. Li, Antibacterial and antioxidant activities of sodium starch octenylsuccinate-based Pickering emulsion films incorporated with cinnamon essential oil, Int. J. Biol. Macromol. 159 (2020) 696–703.
[16] S. Wu, B. Zhang, Y. Liu, X. Suo, H. Li, Influence of surface topography on bacterial adhesion: a review (review), Biointerphases 13 (2018), 060801, .
[17] Jafar Hasan, Kaushik Chatterjee, Recent advances in engineering topography mediated antibacterial surfaces, Nanoscale 7 (2015) 15568–15575.
[18] Hao Song, Yusilawati Ahmad Nor, Meihua Yu, Yannan Yang, Jun Zhang, Hongwei Zhang, Chun Xu, Neena Mitter, Chengzhong Yu. Silica nanopollens enhance adhesion for long-term bacterial inhibition. J. Am. Chem. Soc. 138(2016)6455–62.
[19] Adriana San-Miguel, Sven H. Behrens, Influence of nanoscale particle roughness on the stability of Pickering emulsions, Langmuir 28 (2012) 12038–12043.
[20] Y. Xia, J. Wu, W. Wei, Y. Du, T. Wan, X. Ma, W. An, A. Guo, C. Miao, H. Yue, S. Li, X. Cao, Z. Su, G. Ma, Exploiting the pliability and lateral mobility of Pickering emulsion for enhanced vaccination, Nat. Mater. 17 (2018) 187–194.
[21] Xie, J., Luo, Y., Chen, Y., Liu, Y., Ma, Y., Zheng, Q., Yue, P., Yang, M.. Redispersible Pickering emulsion powder stabilized by nanocrystalline cellulose combining with cellulosic derivatives. Carbohydr. Polym., 213(2019)128–137.
[22] X. Li, J. Zhu, Y. Pan, R. Meng, B. Zhang, H. Chen, Fabrication and characterization of pickering emulsions stabilized by octenyl succinic anhydride -modified gliadin nanoparticle, Food Hydrocoll. 90 (2019) 19–27.
[23] L. Bai, W. Xiang, S. Huan, O.J. Rojas, Formulation and stabilization of concentrated edible oil-in-water emulsions based on electrostatic complexes of a food-grade cationic surfactant (ethyl lauroyl arginate) and cellulose nanocrystals, Biomacromolecules 19 (2018) 1674–1685.
[24] Y. Habibi, L.A. Lucia, O.J. Rojas, Cellulose nanocrystals: chemistry, self-assembly, and applications, Chem. Rev. 110 (2010) 3479–3500.
[25] J.C. Natterodt, J. Sapkota, E.J. Foster, C. Weder, Polymer nanocomposites with cellulose nanocrystals featuring adaptive surface groups, Biomacromolecules 18 (2017) 517–525.
[26] Hu, Z., Patten, T., Pelton, R., Cranston, ED. Synergistic stabilization of emulsions with cellulose nanocrystals and cellulose derivatives. ACS Sustain. Chem. Eng. 3(2015) 1023–1031.
[27] Hu, Z., Ballingerm S., Pelton, R., Cranston, ED. (2015). Surfactant-enhanced cellulose nanocrystal Pickering emulsions. J. Colloid Interface Sci.. 4399(2015) 139–148.
[28] C. Wen, Q. Yuan, H. Liang, F. Vriesekoop, Preparation and stabilization of D-limonene Pickering emulsions by cellulose nanocrystals, Carbohydr. Polym. 112 (2014) 695–700.
[29] G.H. Zhao, N. Kapur, B. Carlin, E. Selinger, J.T. Guthrie, Characterisation of the interactive properties of microcrystalline cellulose-carboxymethyl cellulose hydrogels, Int. J. Pharm. 415 (2011) 95–101.
[30] McClements, D. J. (2015). Food Emulsions: Principles, Practices, and Techniques. CRC press.
[31] Y. He, F. Wu, X. Sun, R. Li, Y. Guo, C. Li, L. Zhang, F. Xing, W. Wang, J. Gao, Factors that affect Pickering emulsions stabilized by graphene oxide, ACS Appl. Mater. Interfaces 5 (2013) 4843.
[32] Y. Zhou, S. Sun, W. Bei, M.R. Zahi, Q. Yuan, H. Liang, Preparation and antimicrobial activity of oregano essential oil Pickering emulsion stabilized by cellulose nanocrystals, Int. J. Biol. Macromol. 112 (2018) 7–13.
[33] D. Eric, Hydrocolloids as emulsifiers and emulsion stabilizers, Food Hydrocoll.. 23 (2009)1473–1482.
[34] S. Varanasi, L. Henzel, L. Mendoza, R. Prathapan, W. Batchelor, R. Tabor, Pickering emulsions electrostatically stabilized by cellulose nanocrystals. Frontiers in Chemistry 6(2018) 409.
[35] L. Bai, S. Lv, W. Xiang, S. Huan, DJ. McClements, OJ Rojas. Oil-in-water Pickering emulsions produced via microfluidization with cellulose nanocrystals: 1. Formation and stability. Food Hydrocoll. 96 (2019) 699–708.
[36] B. Horváth, S. Pál, A. Széchenyi. Preparation and in vitro diffusion study of essential oil Pickering emulsions stabilized by silica nanoparticles. Flavour Fragr J. 33(2018) 1–12.
[37] Y. Ahmad Nor, Y. Niu, S. Karmakar, L. Zhou, C. Xu, J. Zhang, H. Zhang, M. Yu, D. Mahony, N. Mitter, MA. Cooper, C. Yu, Shaping nanoparticles with hydrophilic compositions and hydrophobic properties as nanocarriers for antibiotic delivery. ACS Central Science 1(2015) 328–334.